

Characteristics of human voice vibrations based on FBG strains

Rani Nurpadilla¹, Bunga Meyzia¹, Saktioto^{1,2,*}, Mohammed M Fadhali^{3,4}

¹Department of Physics, Universitas Riau, Pekanbaru 28293, Indonesia

²Nuclear Radiations Laboratory, University of Illinois Urbana-Champaign, Urbana 61801, United States

³Department of Physics, Jazan University, Jazan 45142, Saudi Arabia

⁴Department of Physics, Ibb University, Ibb 70270, Yemen

ABSTRACT

FBG is widely developed as a sensor in its application as a sensor, FBG is commonly used either in industry or in clinical applications to measure changes in physical parameters such as pressure, strain, temperature, and corrosion, as well as to monitor the body's heartbeat and breathing. This research uses 2 types of FBG, namely uniform and chirping. The spectrum used is in the range of 1550 nm. Using an optical sensing interrogator as a tool to read wavelength changes as well as input and output with an infrared laser light source. This study aims to analyze the response of FBG sensors to human voice vibrations with variations in the intensity of sound violence. The results showed that at a hardness intensity of 60 dB using a uniform FBG with a reflectivity of 10% experienced a wavelength change of -0.0304 nm, at an intensity of 70 dB 0.0304 nm, and an intensity of 80 dB experienced many wavelength changes 0.06669 nm. The greater the intensity of the sound, the more FBG response shows an increase in wavelength. The largest strain value detected by the uniform FBG with 10% reflectivity is at 70 dB intensity of 5.5579×10^{-5} strain while the lowest value is at 80 dB intensity of 4.4816×10^{-5} strain. The chirping FBG with 10% reflectivity has the highest strain value at 70 dB intensity with a respective strain value of 1.18×10^{-4} strain. Giving sound vibrations such as some of A, I, U, E, and O to FBG is useful for calculating how the transmission peak of FBG shifts due to strain. When the object emits sound vibrations with a certain intensity, the pressure that occurs will be more than the object when it is at rest, so the greater the sound vibration, the greater the strain that occurs.

ARTICLE INFO

Article history:

Received Nov 28, 2023

Revised Jan 29, 2024

Accepted Feb 20, 2024

Keywords:

Chirped FBG
FBG Uniform
Fiber Bragg Grating
Optical Interrogator
Strain

This is an open access article under the [CC BY](#) license.



* Corresponding Author

E-mail address: saktioto@lecturer.unri.ac.id

1. INTRODUCTION

Vibration is one of the effects that occurs due to movement caused by differences in pressure and frequency [1-4]. Movement can be in the form of continuously decreasing impacts or other words it can also be irregular or random movement [5, 6]. As times change and develop increasingly rapidly, sensor technology is being developed a lot [7-10]. Especially for sound sensors, sound detection is still developing [11, 12]. Sound sensors have developed in various forms, for example, automatic door opening sensors, sound detection on CCTV, vacuum cleaner cleaning command tools, and there are still many uses for sound sensors today [13-19].

Fiber Bragg grating (FBG) is a type of optical fiber that has several gratings in the core that are arranged periodically [20, 21]. FBG is widely applied as a sensor by utilizing the sensitivity of the FBG lattice to strain and temperature [22-25]. This research has studied the application of FBG as a vibration sensor based on its sensitivity to strain.

This research was carried out by identifying human voice vibrations using a combination of FBG sensors with uniform and chirping types which have a reflectivity of 10%, 30%, 50%, 70%, and

90%. This FBG sensor will be measured combined and compared with the FBG wavelength shift. This design will use strain parameters so that analytical calculations are obtained. Using variations of 5 vowels (A, I, U, E, and O) with constant frequency. The Decibel-X application is used to constantize sound by using sound loudness samples of 60, 70, and 80 dB. Then varied with the distance between the sensor and the sound source between 1 cm and 3 cm. Next, it was analyzed using the Sigmaplot and Microsoft Excel applications.

2. RESEARCH METHODS

This research was carried out by identifying human voice vibrations using a combination of FBG sensors with uniform and chirping types which have a reflectivity of 10%, 30%, 50%, 70%, and 90%. This FBG sensor will be measured and used as a combination and compared to the shift in wavelength of the FBG optical fiber, the accuracy, and precision of the sensor in responding to human voice vibrations (see Figure 1). This design will use strain parameters so that analytical calculations are obtained. Using variations of 5 vowels (A, I, U, E, and O) with constant frequency. The Decibel-X application is used to constantize sound by using sound loudness samples of 60, 70, and 80 dB. Then varied with the distance between the sensor and the sound source between 1 cm and 3 cm. Next, each sound spectrum obtained was analyzed. The FBG sensor will be attached using a skin adhesive that is safe from interference, where the human neck is the object that will pick up sound vibrations. Wavelength changes are seen through an interrogator that is connected to the FBG. When producing sound, the object is directed to use the Decibel-X application so that the sound output becomes stable/constant. The object will sound for 10 seconds and will be silent for 5 seconds. Measurements are carried out for 45 seconds, then the data is taken and the wavelength graph is saved.

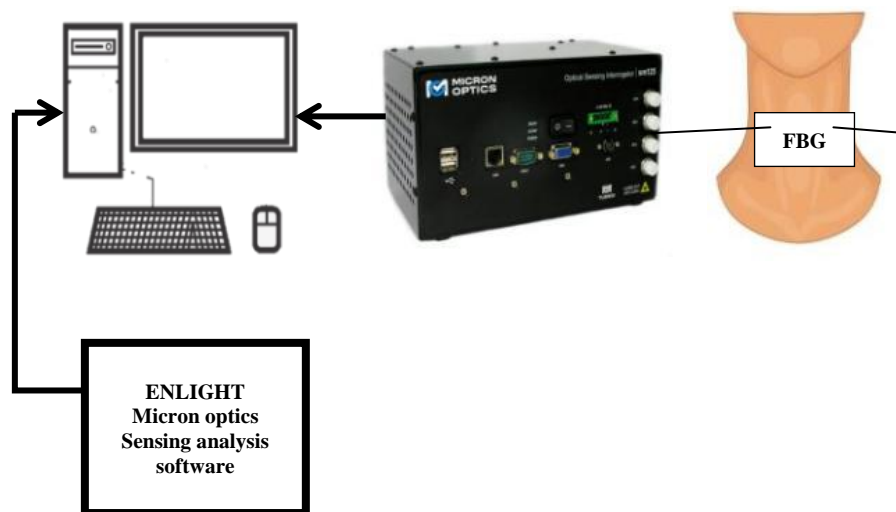


Figure 1. FBG sensor placement scheme.

3. RESULTS AND DISCUSSIONS

3.1. Uniform FBG Wavelength Shift in Human Voice Vibrations

The Bragg wavelength shift is known when the intensity is passed through the FBG to the object. This research uses an edge filter interrogation system method which is used as an interrogator. This system functions to convert changes in the FBG reflection spectrum into changes in power detected by the detector. Apart from that, this system can also be used to see changes in strain that occur. The value of the change in strain will be linear with the change in power.

The difference in peak wavelength difference at an intensity of 60 dB is $\Delta\lambda = -0.0304$ nm. This proves that the greater the vibration given, the greater the change in wavelength. However, because it uses 10% reflectivity, FBG is considered less sensitive in detecting intensities at 60 dB. At an intensity of 70 dB, it is $\Delta\lambda = 0.0492$ nm, while at an intensity of 80 dB, the change is $\Delta\lambda = 0.06669$ nm (see Figure 2).

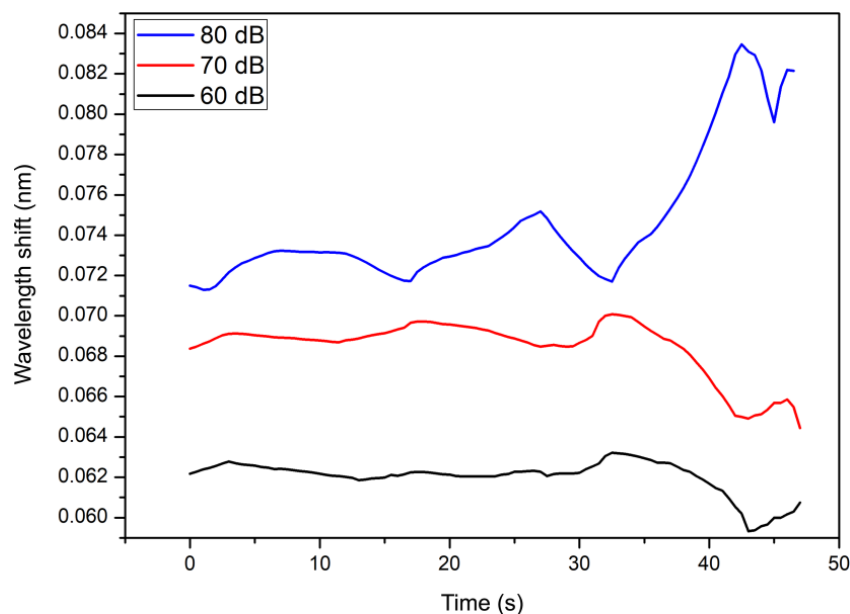


Figure 2. Wavelength shift of uniform FBG with reflectivity 10% variation in sound intensity.

3.2. Wavelength Shift of Chirped FBG to Human Voice Vibrations

The change in Bragg wavelength increases at an intensity of sound vibrations of 80 dB, while the change in wavelength decreases at an intensity of 60 dB (see Figure 3). This happens because the FBG sensor detects human breathing when making sounds. Because during research the object carries out respiration. This shows the similarity of the response of the two FBGs undergoing a stretching process which will cause a change in the Bragg wavelength λ due to changes in the effective refractive index (n_{eff}) and changes in the distance between the Bragg gratings (Δ).

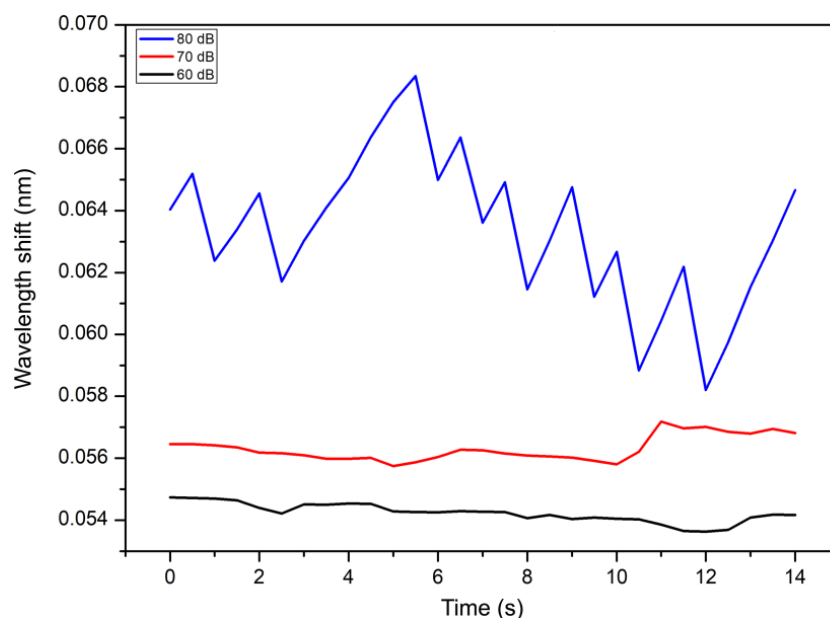


Figure 3. Wavelength shift of chirped FBG reflectivity 10% variation in sound intensity.

Chirped FBG can detect details because the chirped sensor has high sensitivity compared to uniform FBG so the chirped FBG image shows an irrelevant peak-to-peak relationship as a respiratory response with $\Delta\lambda$ which changes over time. From the results obtained, the sensor that can detect sound vibration patterns, as well as breathing patterns, is the chirped FBG. Apart from that, the waveform

produced by the FBG almost matches the waves taken in the Decibel-X application. It can be concluded that the FBG sensor can detect sound vibrations accurately.

3.3. Changes in FBG Sensor Strain to Human Voice Vibrations

Shows the results of strain measurements produced by a uniform FBG with a reflectivity of 10% using the vowels A, I, U, E, and O, from the results obtained the largest strain detected by the FBG was at an intensity of 70 dB of $5.5579 \times 10^{-5} \epsilon$ (strain) while the lowest value is at an intensity of 80 dB with a value of $4.4816 \times 10^{-5} \epsilon$. For the letters, A, I, U, E, and O, the largest and smallest strains show the same results, namely at intensities of 70 dB and 80 dB. However, it shows different strain values. For the vowel letter A the intensity of 60 dB has a strain value of $5.1652 \times 10^{-5} \epsilon$. The vowel E has a large stretch value of $5.5770 \times 10^{-5} \epsilon$ and the vowel O has a stretch value of $5.7871 \times 10^{-5} \epsilon$ (see Figure 4).

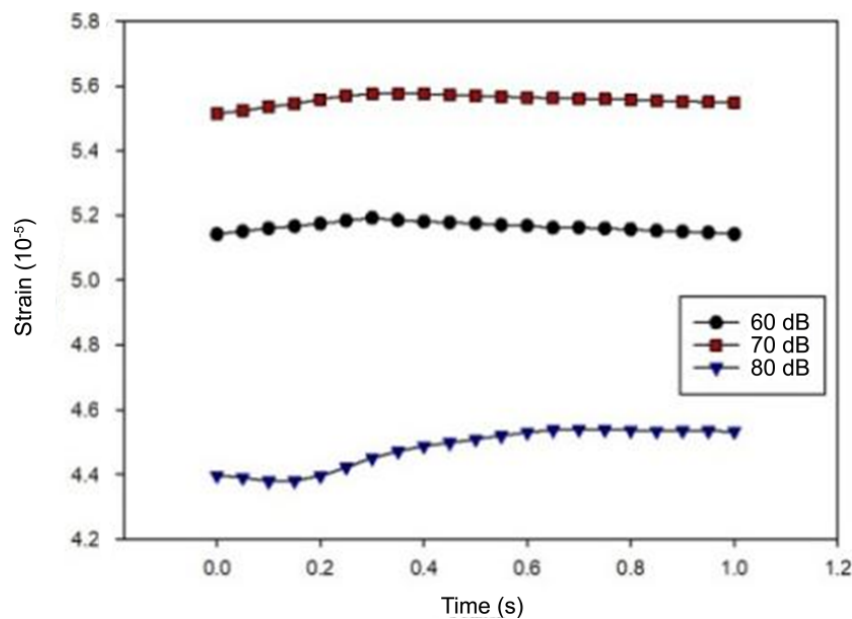


Figure 4. Change in 10% uniform FBG strain with variations in sound intensity.

Uniform FBG with 10% reflectivity detects the intensity of 60 different strain values but the 60 dB intensity graph is in the middle between 70 dB and 80 dB. Vowel strain values for an intensity of 60 dB show different results.

3.4. Changes in Chirped FBG Sensor Strain to Human Voice Vibrations

Strain obtained using FBG Chirping with a reflectivity of 10% for the vowels A and I the highest strain value at an intensity of 70 dB with respective strain values of $1.18 \times 10^{-4} \epsilon$ and $8.91 \times 10^{-5} \epsilon$ these results are the same as the results strain data obtained by uniform FBG (see Figure 5). Meanwhile, for the vowels U, E, and O the highest strain values show an intensity of 80 dB with respective strain values of $1.11 \times 10^{-4} \epsilon$, $8.18 \times 10^{-5} \epsilon$, and $1.11 \times 10^{-5} \epsilon$. However, for the vowels E and O the graph experiences tangency at intensities of 60 and 70 dB. This is due to several factors such as detection errors on the FBG sensor, signal quality can be damaged by external movements made by objects. This error can be caused by high sensor sensitivity. This sensitivity becomes a problem when the object being monitored for example breathes and changes position, makes additional movements, coughs, etc.

Providing sound vibrations to the FBG is useful for calculating how much the transmission peak of the FBG shifts due to strain. When an object emits sound vibrations with a certain intensity, the pressure that occurs will be greater than when the object is at rest, so the greater the sound vibration, the greater the strain that occurs. However, when emitting sound vibrations, many other factors influence the object which can also influence the strain results obtained.

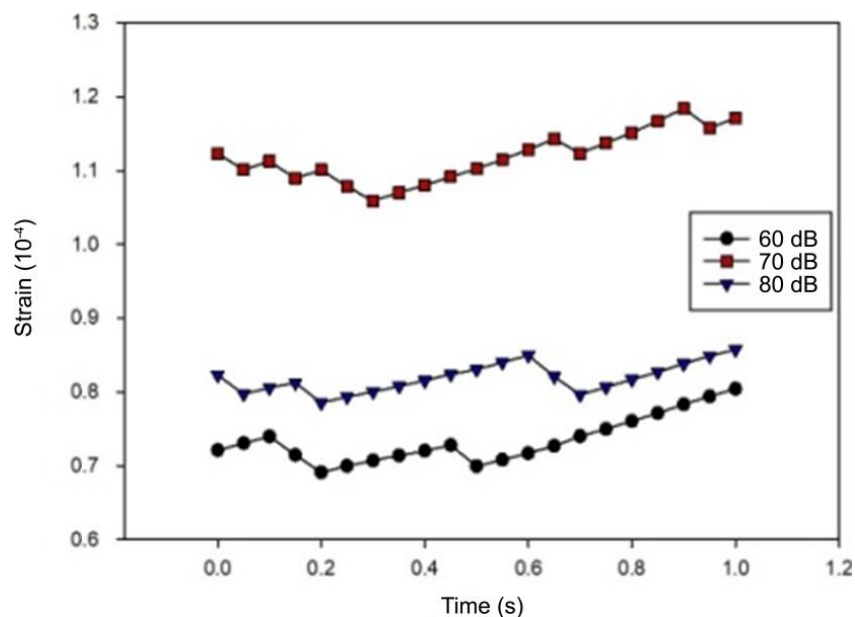


Figure 5. Changes in 10% chirped FBG strain with variations in sound intensity.

4. CONCLUSION

Based on the measurement results, it can be concluded that the human body temperature system sensor series using FBG chirping is more sensitive in detecting strains and shifts in the wavelength of human sound vibrations.

REFERENCES

- [1] Hikma, N., Saktioto, T., & Soerbakti, Y. (2023). Vibration analysis of diaphragmatic breathing activity using single-mode fiber and fiber Bragg grating. *AIP Conference Proceedings*, **2858**(1).
- [2] Bartel, L. & Mosabbir, A. (2021). Possible mechanisms for the effects of sound vibration on human health. *Healthcare*, **9**(5), 597.
- [3] Zairmi, Y., Basdyo, D., Hairi, H. M., Abd Aziz, M. S., & Abdullah, H. Y. (2022). Inspection of birefringence characteristics to establish single-mode fiber quality. *Science, Technology and Communication Journal*, **2**(3), 91–96.
- [4] Peixin, G. A. O., Tao, Y. U., Zhang, Y., Jiao, W. A. N. G., & Jingyu, Z. H. A. I. (2021). Vibration analysis and control technologies of hydraulic pipeline system in aircraft: A review. *Chinese Journal of Aeronautics*, **34**(4), 83–114.
- [5] Alatawi, A. & Reardon, P. J. (2014). Absolute interferometric test of cylindrical wavefront with a fiber optic. *Optical Engineering*, **53**(11), 114104.
- [6] Animasaun, I. L., Ibraheem, R. O., Mahanthesh, B., & Babatunde, H. A. (2019). A meta-analysis on the effects of haphazard motion of tiny/nano-sized particles on the dynamics and other physical properties of some fluids. *Chinese Journal of Physics*, **60**, 676–687.
- [7] Saktioto, T., Defrianto, D., Hikma, N., Soerbakti, Y., Syamsudhuha, S., Irawan, D., ... & Hanto, D. (2022). Airflow vibration of diaphragmatic breathing: model and demonstration using optical biosensor. *TELKOMNIKA (Telecommunication Computing Electronics and Control)*, **21**(3), 667–674.
- [8] Erlinda, S., Veriyanti, V., Saktioto, S., & Abdullah, H. Y. (2022). The effect of light waves on polarization mode dispers. *Science, Technology and Communication Journal*, **2**(2), 49–54.
- [9] Chadha, U., Bhardwaj, P., Agarwal, R., Rawat, P., Agarwal, R., Gupta, I., Panjwani, M., Singh, S., Ahuja, C., Selvaraj, S. K., Banavoth, M., Sonar, P., Badoni, B., & Chakravorty, A. (2022). Recent progress and growth in biosensors technology: A critical review. *Journal of Industrial and Engineering Chemistry*, **109**, 21–51.
- [10] Javid, M., Haleem, A., Singh, R. P., Rab, S., & Suman, R. (2021). Significance of sensors for industry 4.0: Roles, capabilities, and applications. *Sensors International*, **2**, 100110.

- [11] Saktioto, S., Defrianto, D., Hikma, N., Soerbakti, Y., Irawan, D., Okfalisa, O., Widiyatmoko, B., & Hanto, D. (2022). External perspective of lung airflow model via diaphragm breathing sensor using fiber optic belt. *The 4th Al-Noor International Conference for Science and Technology*, **4**(1), 1014.
- [12] Su, T., Liu, N., Lei, D., Wang, L., Ren, Z., Zhang, Q., Su, J., Zhang, Z., & Gao, Y. (2022). Flexible MXene/bacterial cellulose film sound detector based on piezoresistive sensing mechanism. *ACS Nano*, **16**(5), 8461–8471.
- [13] Fidanboylyu, K. & Efendioglu, H. S. (2009). Fiber optic sensors and their applications. *5th International Advanced Technologies Symposium (IATS'09)*, **6**, 2–3.
- [14] Maulana, A. M., Ramadhan, K., & Irawan, D. (2023). Analysis of fluid flow in a cylindrical tube using fiber Bragg grating. *Science, Technology and Communication Journal*, **4**(1), 17–22.
- [15] Azizah, Y. N., Candra, W., & Fadhali, M. M. (2022). Characteristics of fiber Bragg grating due to temperature changes in honey solution. *Science, Technology and Communication Journal*, **2**(2), 63–68.
- [16] Fitri, A., Candra, W., & Meyzia, B. (2021). Determination of optical parameters on knee bending of the feet using fiber optic. *Science, Technology and Communication Journal*, **2**(1), 9–14.
- [17] Cai, C., Zheng, R., & Luo, J. (2022). Ubiquitous acoustic sensing on commodity iot devices: A survey. *IEEE Communications Surveys and Tutorials*, **24**(1), 432–454.
- [18] Javid, M., Haleem, A., Rab, S., Singh, R. P., & Suman, R. (2021). Sensors for daily life: A review. *Sensors International*, **2**, 100121.
- [19] Fu, B., Damer, N., Kirchbuchner, F., & Kuijper, A. (2020). Sensing technology for human activity recognition: A comprehensive survey. *IEEE Access*, **8**, 83791–83820.
- [20] Ramadhan, K., Irawan, D., & Yupapin, P. (2023). Core multi-layer dispersion on single-mode optical fiber. *Science, Technology and Communication Journal*, **3**(3), 89-94.
- [21] Mishra, M. & Sahu, P. K. (2023). Fiber Bragg gratings in healthcare applications: A review. *IETE Technical Review*, **40**(2), 202–219.
- [22] Bader, R., Pagel, T., Renner, H., & Brinkmeyer, E. (2011). Characterization of chirped fiber Bragg gratings: identification and removal of cladding-mode perturbations in measurement data. *Journal of lightwave technology*, **29**(12), 1783–1789.
- [23] Basdyo, D., Zairmi, Y., & Yupapin, P. (2022). Non-concentric single-mode optical fiber dispersion. *Science, Technology and Communication Journal*, **3**(1), 7-12.
- [24] Boateng, E. K. G., Schubel, P., & Umer, R. (2019). Thermal isolation of FBG optical fibre sensors for composite cure monitoring. *Sensors and Actuators A: Physical*, **287**, 158–167.
- [25] Khan, R. Y. M. & Faisal, M. (2023). Fiber Bragg Grating Temperature Sensor and its Interrogation Techniques. *Journal of Brilliant Engineering*, **3**, 4840.